

CFD Modeling of Supersonic Airflow Generated by 2D Nozzle With and Without an Obstacle at the Exit Section

Olivera P. Kostić

Research Assistant
University of Belgrade
Faculty of Mechanical Engineering
Innovation Centre

Zoran A. Stefanović

Full Professor
University of Belgrade
Faculty of Mechanical Engineering

Ivan A. Kostić

Associate Professor
University of Belgrade
Faculty of Mechanical Engineering

Computational modeling of complex supersonic airflow patterns is one of the greatest challenges in the domain of CFD analyses. The paper presents initial steps in numerical analysis of such flow, generated by convergent-divergent nozzle with Mach number $M = 2.6$ at nozzle exit. The aim was to achieve good agreements with available experimental data, obtained during supersonic wind tunnel tests at VTI Žarkovo institute, where nozzle thrust vectoring possibilities had been investigated using air as test fluid, by placing different types of obstacles at the exit section. Paper is focussed on free exit flow, and flow with one selected obstacle type. Using structured mesh for both cases, the RANS equations with $k-\omega$ SST turbulent model have been applied. After quantitative and qualitative comparisons with available experimental data, good agreements have been obtained, where CFD was also able to provide additional flowfield data, not measured during experiments.

Keywords: supersonic nozzle, flow vectoring by obstacles, CFD analysis, RANS $k-\omega$ SST, pressure distribution, flow visualization.

1. INTRODUCTION

This paper presents the most relevant aspects of the numerical analysis of airflow inside and behind the convergent-divergent nozzle with supersonic exhaust, performed for two cases: without, and with a mechanical obstacle in exit section of the nozzle.

The starting point of here presented numerical analyses were wind tunnel tests [1], [2], [3] performed in VTI Žarkovo (Belgrade) by the joint team from the Faculty of Mechanical Engineering, University of Belgrade and Aeronautical Technical Institute Žarkovo, as a part of experimental research of methods used for thrust vector control on modern rocket engines. This approach implies deflection of supersonic outcoming stream using a mechanical obstacle at the nozzle exit section in order to change the thrust vector direction, without moving the whole nozzle (different approaches are discussed in [4], [5]). In these experiments, the test fluid was air, and tests were performed with a variety of different obstacle shapes, positions and sizes (one example is shown in Fig. 1).

The ability to numerically simulate the same test conditions, geometry and results, gives researchers a chance to spread the investigation to many other possible obstacle forms and shapes, without performing expensive wind tunnel tests. The first step in this direction is proper software “calibration”, i.e. the definition of optimum computational tools that will reproduce experimental results, both in qualitative and quantitative sense, with satisfactory level of accuracy.

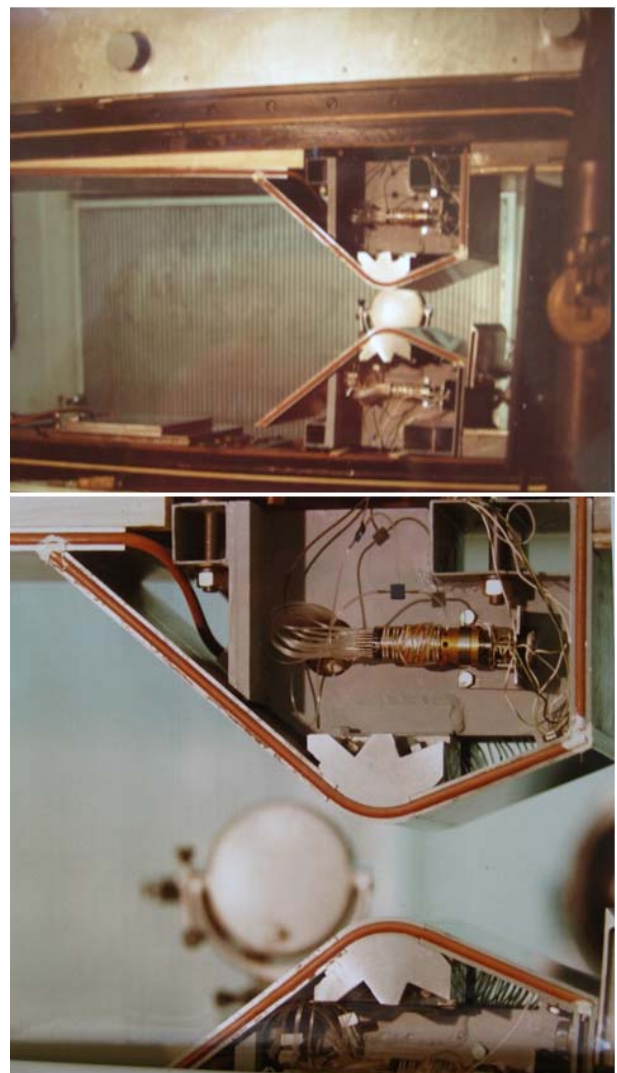


Figure 1. Test section of the wind tunnel with convergent - divergent nozzle for $M = 2.6$, with high positioned obstacle at the outlet (airflow from left to right)

Received: July 2014, Accepted: August 2014

Correspondence to: Dr Ivan Kostić
Faculty of Mechanical Engineering,
Kraljice Marije 16, 11120 Belgrade 35, Serbia
E-mail: ikostic@mas.bg.ac.rs

doi:10.5937/fmet1502107K

© Faculty of Mechanical Engineering, Belgrade. All rights reserved

FME Transactions (2015) 43, 107-113

107

Initial CFD simulations, presented in this paper, have been performed for nominal Mach number $M = 2.6$ at the nozzle exit, first for free exit section, and then with 15 mm high obstacle at exit bottom side, resembling airflow parameters from both experiments (recent investigations and results considering these problems can be found, for example, in [6], [7], [8]).

Results obtained using CFD analysis were then compared with available experimental data in order to validate applied methodology for the simulation of very complex supersonic flow field inside and behind the nozzle.

2. EXPERIMENTAL FACILITY AND AIRFLOW CONDITIONS

Tests were performed in T-36 indraft supersonic wind tunnel in Military Technical Institute VTI Žarkovo, using scaled model [9] of convergent-divergent nozzle with rectangular cross-section and air as a working fluid. In spite of the presence and certain influence of side walls, such tests are treated as 2D flow category.

Experimental 2D model of the nozzle with obstacle at the outlet, positioned in test section of the wind tunnel is shown in Fig. 1. The geometry that was used in tests with nominal Mach number $M = 2.6$ at the nozzle exit [1], [10] has been applied for the generation of CFD control volume (dimensions are shown in Fig. 2).

Pressure in vacuum tank for all tests was of the order of 5 mbar, while inlet values slightly varied depending on ambient conditions. For example, for one of the tests with 15 mm obstacle (exact value is 15.52 mm), the parameters were [1]:

- atmospheric pressure 1018.313 mbar, and
- atmospheric temperature 286.75 K, which further influenced other parameters, such as:
- reference Mach number 0.086, achieved in test installation in front of the nozzle,
- total pressure in wind tunnel test section 1010.542 mbar, etc.

In CFD calculations, for proper comparisons with the experiment, actual test values were applied for assigning the inlet and outlet conditions and parameters.

Measurement points for pressure distribution readings were positioned in characteristic zones along the nozzle walls and the obstacle, grouped in three zones. In this paper, pressure readouts in zone on upper and lower divergent section walls, in the plane of symmetry, were used for comparisons.

Visualisation of the flow field during experiments was done by colour Schlieren photographs. Since they will be used for comparisons with CFD results, it should be noted that these photos provide “inverted” colours on upper and lower side of the picture, although – in case of tests without obstacles, flow fields in these domains are symmetrical (and so are the shapes captured on photos, but colours are not - see for example Fig. 5).

3. CALCULATION PROCEDURE

Numerical analyses were done applying 2D flow modelling in ANSYS Fluent 14. Control volume dimensions used in these calculations are shown in Fig.

2. Also, in this paper only the influence one type of wedge-shaped obstacle has been analyzed, protruding 15.52 mm inside the exit section, and without gap between the obstacle and exit section’s lower wall.

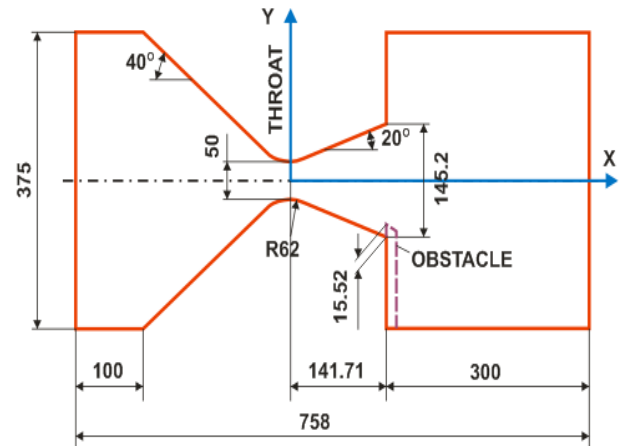


Figure 2. Geometry of the control volume applied in CFD calculations (dimensions are in millimetres)

For both cases static structured meshes were used. Attention was paid to appropriate control volume segmenting, edge sizing and application of appropriate bias type and factor, in order to increase the number of elements in critical calculation domains such as walls, sharp wall and obstacle edges etc., but still keep the total number of elements at reasonably low values, with satisfactory mesh quality. The outcome is shown in Figs 3 and 4, where total number of elements for both cases is of the order of 195000.

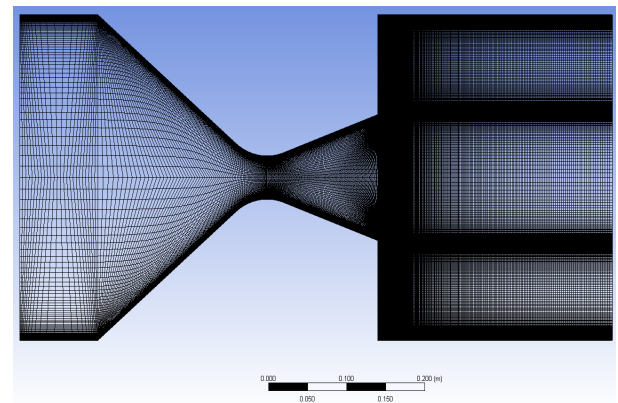


Figure 3. Structured mesh for the calculation of airflow without the obstacle at nozzle exit

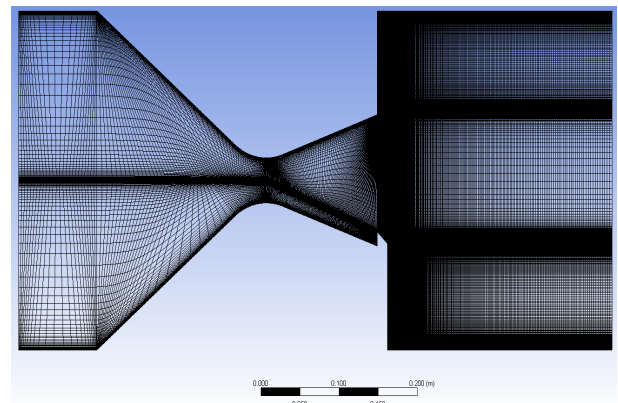


Figure 4. Structured mesh for the calculation of airflow with 15 mm obstacle at nozzle exit

The size of aft control volume domain (behind the nozzle), which was initially set to 100 mm, had to be increased to 300 mm (see Fig. 2) in order to obtain proper modelling of trapped flow in corners above and below the nozzle exit domain.

Calculation of flow characteristics inside the adopted control volume were performed using RANS (Reynolds-Averaged Navier-Stokes) equations with $k-\omega$ SST (Shear-Stress Transport) turbulent model [11], [12], [13]. The most important settings that have been applied are:

- Solver: 2D density-based.
- Model: viscous, SST $k-\omega$, with compressibility effects.
- Fluid: air, ideal gas, viscosity by Sutherland law, three coefficient method.
- Boundary conditions: control volume inlet and outlet parameters as defined in [1], for given test case.
- Calculation: flow type – supersonic, FMG - the Full Multi-Grid solution initialization at 4 levels [13], [14], initial optimum reordering of the mesh domain using Reverse Cuthill-McKee method [14], active solution steering, applying automatic optimization of Courant number for the achieved solution convergence stage, etc.

It had been assumed that the solution for the given case has converged when the solution monitor for mass flow rate through the control volume outlet showed no change (and remained constant observing significant number of digits) for at least 100 consecutive iterations.

4. RESULTS AND DISCUSSION

Initial calculations were performed for the case of nozzle without the obstacle at exit section. It should be emphasized that the calculation procedure, described in previous chapter, has been adopted after a series of test runs, when finally both qualitative and quantitative verifications of the method have been obtained, comparing calculated flow characteristics with experimental data.

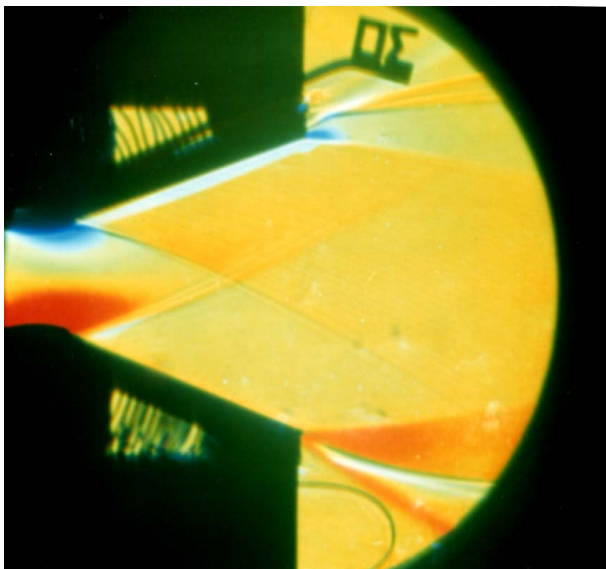


Figure 5. Schlieren photo of airflow through the nozzle, without obstacle at exit section

Schlieren photo of free exit flow, with established Mach number of $M = 2.6$ in exit section, is shown in Fig. 5. Characteristic features for visual comparisons are expansion domains at exit corners, and inclinations of shock waves generated at aft-throat positions, where radial shape in divergent nozzle domain changes to linear.

Figures 6 and 7, obtained in Fluent, show Mach number and dynamic pressure distributions within the control volume. These two flow parameters have been selected for qualitative verifications, because they clearly show the similarities of exit corner expansion domains with Fig. 5, while Fig. 7 well depicts the aft-throat shocks. It should also be noted that Fluent has no capability of generating visualizations similar to Schlieren technique, i.e. proportional to density gradient (and also not with inverted colours in upper and lower flow field domains).

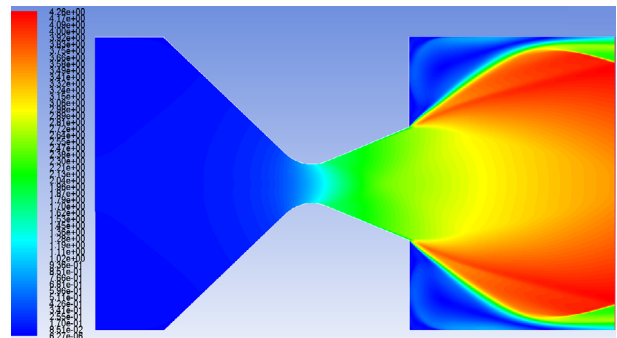


Figure 6. Mach number distribution obtained by CFD calculations for case without obstacle

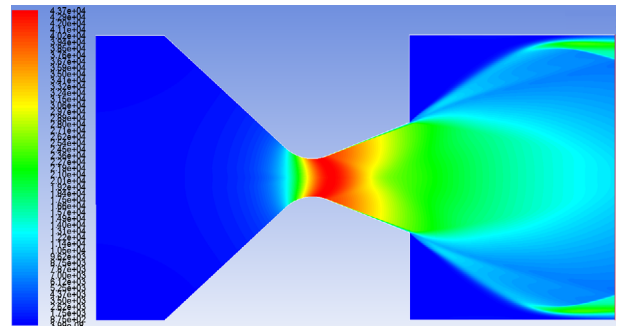


Figure 7. Dynamic pressure distribution obtained by CFD calculations for case without obstacle

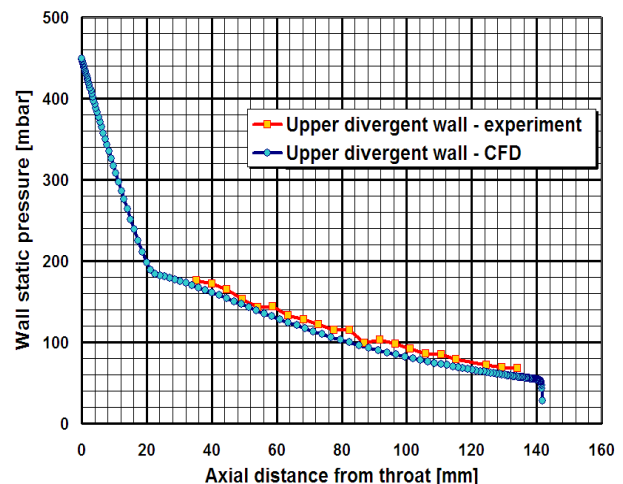


Figure 8. Upper divergent nozzle wall - static pressure comparisons, without obstacle

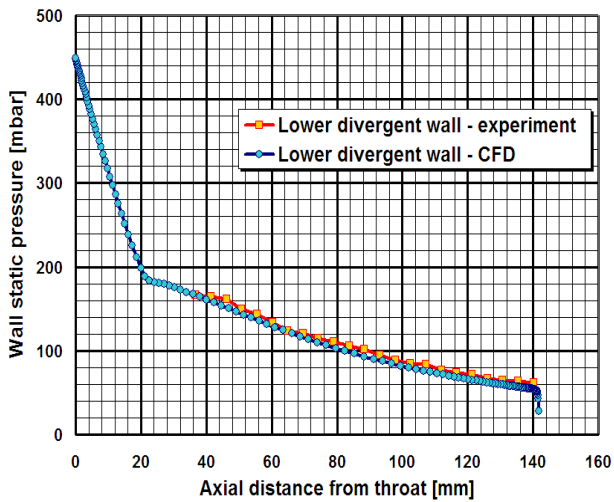


Figure 9. Lower divergent nozzle wall - static pressure comparisons, without obstacle

Quantitative verifications of CFD results were performed by comparing pressure distributions on upper and lower walls in linear divergent nozzle domain.

Figures 8 and 9 show comparisons between experimental and calculated values of wall static pressure on upper and lower side respectively. Although CFD values are slightly smaller than experimental, achieved agreement is quite satisfactory. Also, calculated Mach number at exit section axis is exactly $M = 2.6$ (see Fig.10 and Fig. 21 as well).

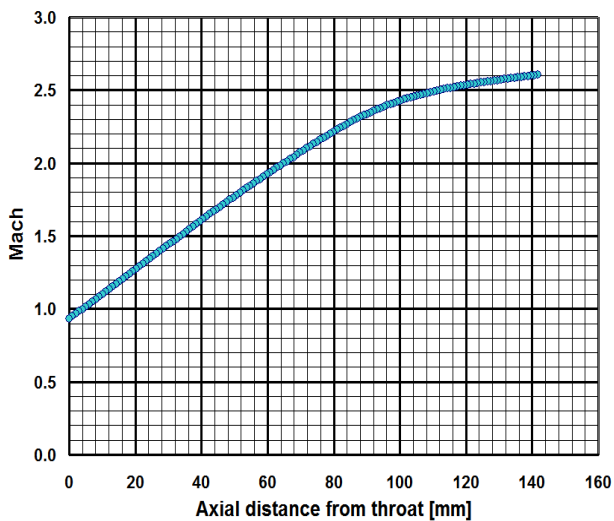


Figure 10. Calculated Mach number along the nozzle axis, from throat to divergent section exit, without obstacle

After verifying the applied calculation model on free exit case, the next step was CFD modeling of the flow with the smallest obstacle used in wind tunnel tests [1]. This was wedge-shaped form, protruding slightly more than 15 mm into the exit section, without the gap between it and lower exit wall (in other tests, this particular obstacle was positioned higher, 30 mm and 45 mm inside the exit, without and with gaps with respect to the wall; these tests will be the subject of future planned CFD analyses). Schlieren photo of this test is shown in Fig. 11, where nominal exit Mach number was also $M = 2.6$. Beside the features mentioned for Fig. 5, additional characteristic features for qualitative

comparisons of CFD with experiment are the oblique shock and trapped zone of fluid in front of the obstacle. Both of them are clearly defined in Figs 12 and 13, obtained by Fluent.

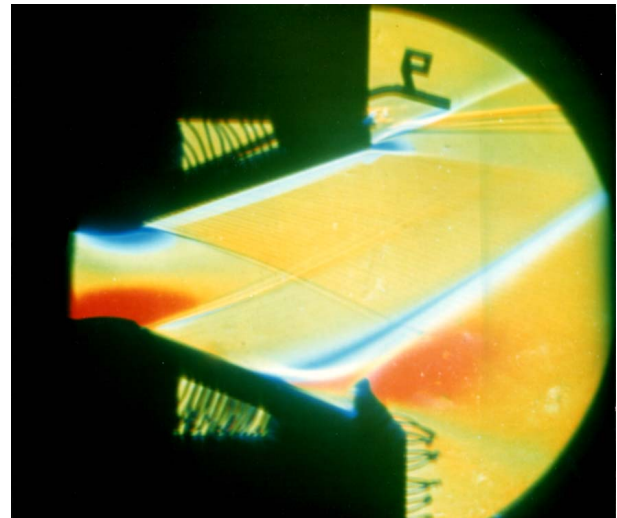


Figure 11. Schlieren photo of airflow with 15 mm obstacle

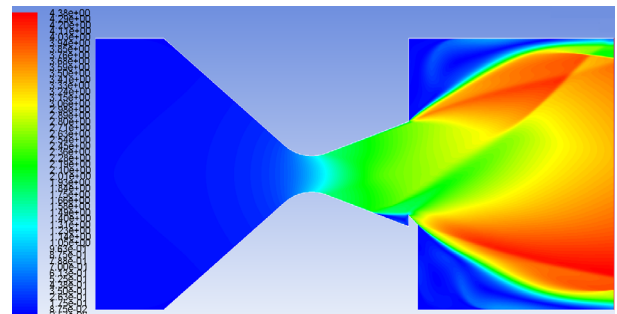


Figure 12. Mach number distribution obtained by CFD calculations for 15 mm obstacle

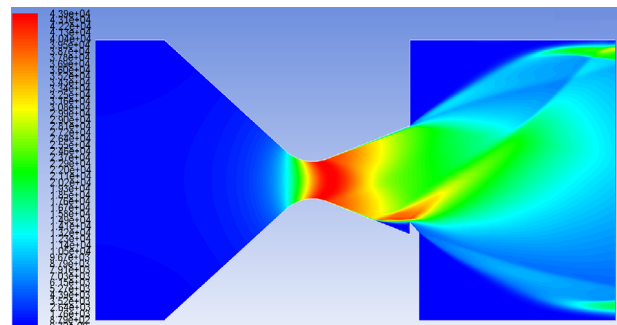


Figure 13. Dynamic pressure distribution obtained by CFD calculations for 15 mm obstacle

Comparison of static pressure on upper divergent wall is given in Fig. 14, showing practically the same level of computational accuracy as in previous case.

In case of lower wall static pressures (Fig. 15), CFD analysis has generally well depicted the oblique shock influence. The difference exists in the near-wall domain where the shock wave is generated. According to experimental measurements (and see Fig. 11 as well), it is generated earlier than predicted by Fluent, and is bent near the wall, causing smoother pressure change. On the other hand, CFD gives abrupt pressure jump. One of the possible explanations is that here presented CFD calculations have been performed with perfectly smooth walls, while on wind tunnel nozzle roughness inevitably

existed, and most probably influenced the shock behavior in the domain close to the wall.

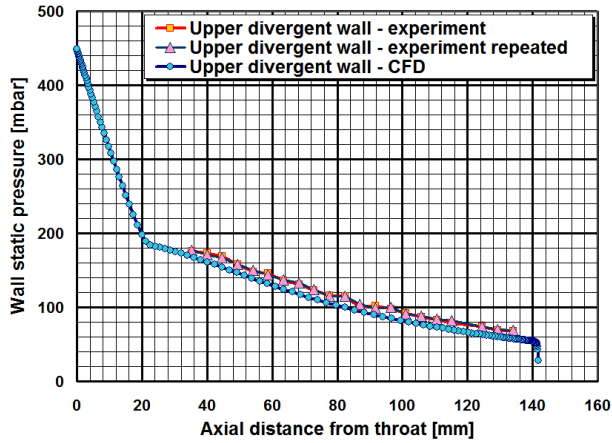


Figure 14. Upper divergent nozzle wall - static pressure comparisons, with 15 mm obstacle

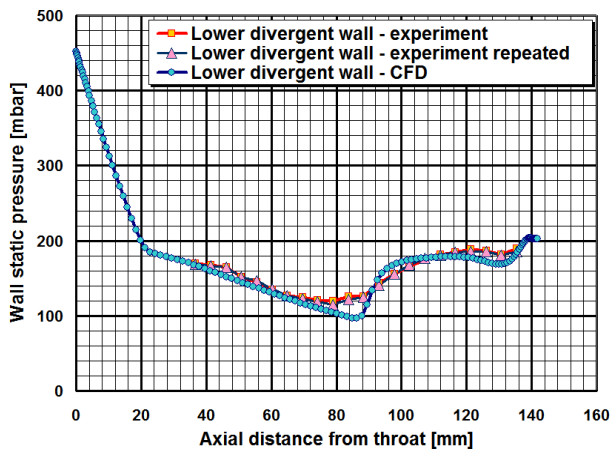


Figure 15. Lower divergent nozzle wall - static pressure comparisons, with 15 mm obstacle

Once the calculation model has been verified by experimental results, meaning that software can be considered “well calibrated”, it can provide many details considering fluid flow characteristics which were not measured during actual wind tunnel tests.

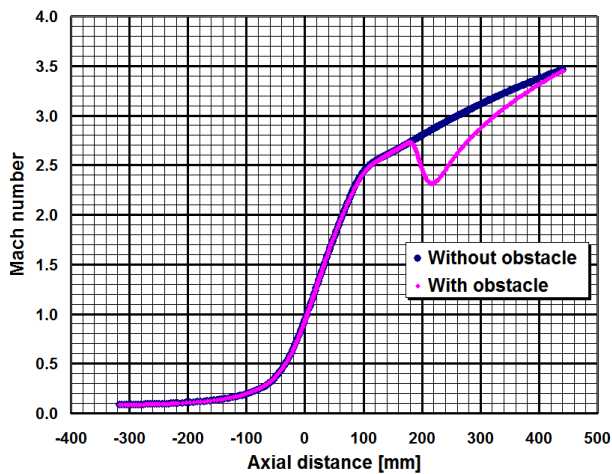


Figure 16. Calculated Mach number along the control volume axis (zero coordinate corresponds to throat)

Some typical examples are shown in the Figs 16 - 19, where values of most relevant fluid flow parameters have been calculated along the entire control volume

axis, with typical changes as they pass through the oblique shock wave, for 15 mm obstacle case.

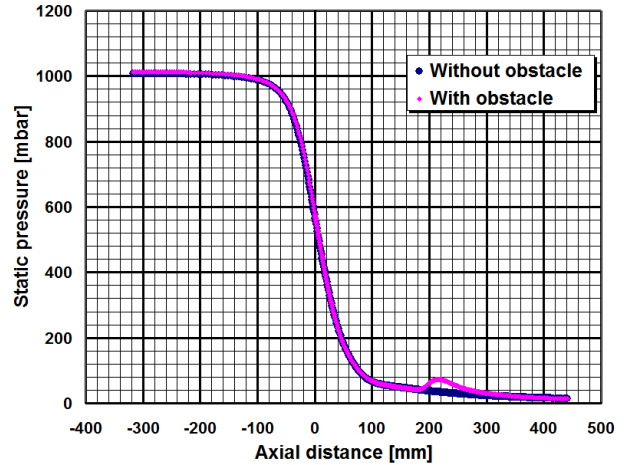


Figure 17. Calculated static pressure along the control volume axis

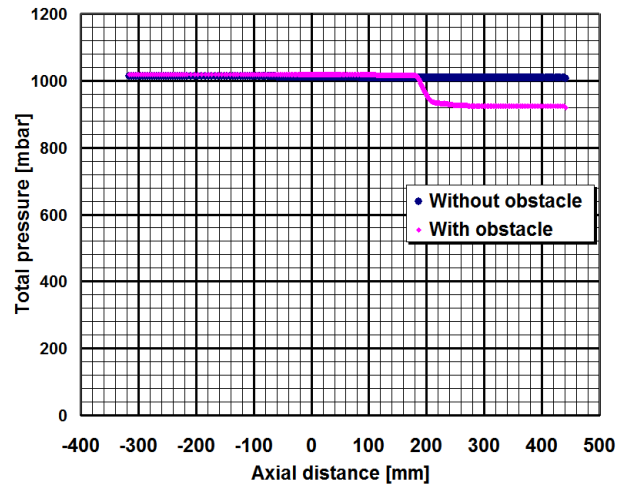


Figure 18. Calculated total pressure along the control volume axis

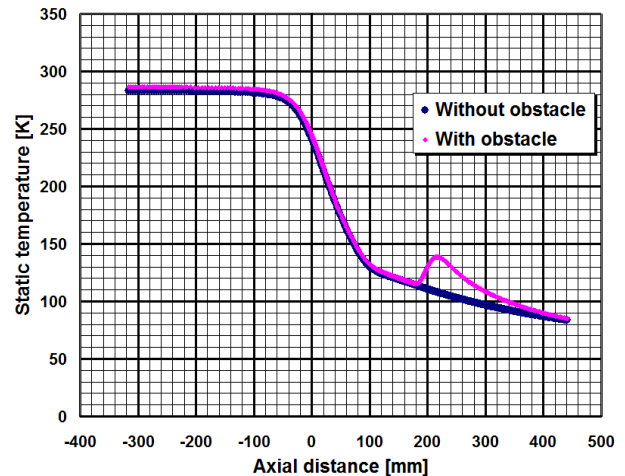


Figure 19. Calculated static temperature along the control volume axis

The vertical profile of Mach number distribution along the exit section height (Fig. 20) has also not been measured in experiments. Calculated values verify that in both tests, the value $M = 2.6$ was achieved at the exit section axis (zero Mach number values correspond to the walls, i.e. to no-slip condition).

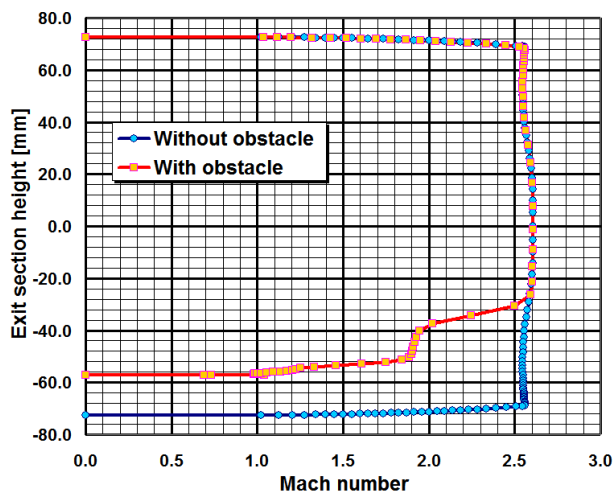


Figure 20. Calculated Mach number vertical profiles along nozzle exit height, for both test cases

Another example is calculated turbulence intensity distribution - Fig. 21 shows the case with obstacle, etc.

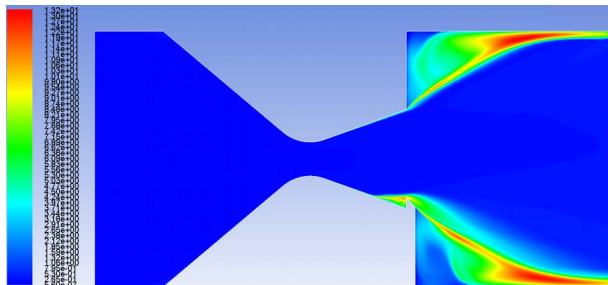


Figure 21. Calculated turbulence intensity in control volume with 15 mm obstacle

More important role of well calibrated software for the given category of problems is the capacity to investigate different kinds of obstacles, that were not previously tested in the wind tunnel, and to perform optimum selection based on much wider investigations. In here presented paper, only one obstacle case has been analyzed. In order to truly verify presented calculation approach, the number of verification cases must be increased and may, and should lead to its further improvements.

5. CONCLUSION

The CFD modelling of two characteristic cases of supersonic flow generated by convergent-divergent nozzle has been done, for free nozzle exit case, and with a selected obstacle. Using static structured meshes for both cases, RANS equations with $k-\omega$ SST turbulent model have been applied, with a properly selected set of additional computational parameters, obtaining stable convergence of the solutions. After comparing numerical results with appropriate experimental data, obtained by supersonic wind tunnel tests, with the same nozzle and obstacle geometry aimed for thrust vectoring, and nominal airflow parameters, good agreements were obtained, both in the qualitative and quantitative sense. These initial CFD investigations will be spread to a large number of obstacles types and sizes for which experimental data exist, in order to verify and further improve the presented calculation approach.

Final aim is to establish a reliable calculation methodology, which could be used for the generation and optimizing of new obstacle types and shapes for thrust vectoring, without the need to perform additional, quite expensive and time consuming wind tunnel tests.

REFERENCES

- [1] Jojić, B., Stefanović, Z., Blagojević, Đ., Vučković, S., Rajčić, Z.: *Research in Modern Rocket Propulsion TVC* (in Serbian), University of Belgrade, Faculty of Mechanical Engineering and VTI Žarkovo, 1984.
- [2] Stefanović, Z., Miloš, M., Todić, I., Pavlović, M.: Investigation of the Pressure Distribution in a 2D Rocket Nozzle with a Mechanical System for Thrust Vector Control (TVC), *Strojarstvo*, Vol. 53 (4), pp 287-292, 2011.
- [3] Jojić, B., Milinović, M., Stefanović, Z., Blagojević, D.: Pressure Distribution in Rocket Nozzle with Mechanical System for TVC, *AIAA Paper 87-1824*, June 1987.
- [4] Nauparac, D., Prsić, D., Miloš, M., Samadžić, M., Isaković, J.: Design Criterion to Select Adequate Control Algorithm for Electro-Hydraulic Actuator Applied to Rocket Engine Flexible Nozzle Thrust Vector Control Under Specific Load, *FME Transactions*, Vol. 41, No. 1, pp. 33-40, 2013.
- [5] Gligorijević, N., Živković, S., Subotić, S., Kozomara, S., Nikolić, M., Čitaković, S.: Side Force Determination in the Rocket Motor Thrust Vector Control System, *Scientific Technical Review*, Vol. 63, No. 1, pp. 27-38, 2013.
- [6] Zmijanović, V., Rašuo, B., Chpoun, A.: Flow Separation Models and Side Phenomena in an Over Expanded Nozzle, *FME Transactions*, Vol. 40, No. 3, pp. 111-118, 2012.
- [7] Živković, S., Milinović, M., Adamec, N.: Experimental and Numerical Research of a Supersonic Planar Thrust Vectoring Nozzle via Mechanical Tabs, *FME Transactions*, Vol. 42, No. 3, pp. 205-211, 2014.
- [8] Natta, P., Kumar, R., Hanumantha, R.: Flow Analysis of Rocket Nozzle Using Computational Fluid Dynamics (CFD), *International Journal of Engineering, Research and Applications*, 2 (5), pp. 1226-1235, 2012.
- [9] Jojić, B., Stefanović, Z.: *Theoretical Analysis and Design of 2D TVC Model for Wind Tunnel Testing* (in Serbian), University of Belgrade, Belgrade, 1983.
- [10] Stefanović, Z.: *Research of Fluid Flow and Pressure Distribution in Supersonic Nozzle in Connection with the Vector Thrust Control*, PhD thesis, University of Belgrade, Belgrade, 1986.
- [11] Wilcox, D. C.: *Turbulence Modelling for CFD*, DCW Industries, Inc., California, USA, 2006.
- [12] ANSYS FLUENT 14.0: *Theory Guide*, ANSYS, Inc., Canonsburg, PA, 2011.

[13] ANSYS FLUENT 14.0: *User's Guide*, ANSYS, Inc., Canonsburg, PA, 2011.

[14] ANSYS FLUENT 14.0: *Tutorial Guide*, ANSYS, Inc., Canonsburg, PA, 2011.

CFD МОДЕЛИРАЊЕ НАДЗВУЧНЕ ВАЗДУШНЕ СТРУЈЕ ГЕНЕРИСАНЕ 2D МЛАЗНИКОМ СА ПРЕПРЕКОМ И БЕЗ ПРЕПРЕКЕ НА ИЗЛАЗУ

Оливера Костић, Зоран Стефановић,
Иван Костић

Моделирање сложених надзвучних струјних поља коришћењем рачунара представља један од највећих изазова у области CFD анализа. У раду су представљени први кораци у нумеричкој анализи таквог струјања, генерисаног конвергентно-дивергентним млазником са Маховим бројем $M =$

2.6 на излазу из млазника. Циљ је био постићи добра поклапања са расположивим експерименталним подацима, добијеним током испитивања у надзвучном аеротунелу института ВТИ Жарково, где су испитиване могућности векторисања потиска млазника са ваздухом као радним флуидом, постављањем различитих типова препрека на излазу из млазника. У раду се анализирају случајеви струјања са слободним излазом и са једним изабраним типом препреке на излазу из млазника. За оба случаја коришћене су структуриране прорачунске мреже за решавање RANS једначина са $k-\omega$ SST турбулентним моделом. Након квалитативних и квантитативних поређења са расположивим експерименталним резултатима, утврђена су добра поклапања, при чему је CFD анализа била у могућности да пружи и додатне податке о струјном пољу, који нису мерени током експеримената.